

Temporal evolution of chlorine monoxide in the middle stratosphere

Philippe Ricaud,¹ Martyn P. Chipperfield,² Joe W. Waters,³ James M. Russell III,⁴ and Aidan E. Roche⁵

Abstract. The temporal evolution of stratospheric chlorine monoxide (ClO) at northern midlatitudes is studied over different scales: diurnal and seasonal variations. Data sets include temperature profiles, and ClO, HCl, ClONO₂, NO₂, O₃, H₂O, and CH₄ mixing ratios as measured from 10 to 0.46 hPa (i.e., from ~30 to ~55 km) by the Microwave Limb Sounder (MLS), by the Halogen Occultation Experiment, and by the Cryogenic Limb Array Etalon Spectrometer instruments aboard the UARS satellite from at most September 1991 to June 1997 within the band 40°–50°N. The time evolution of these species is interpreted by comparison with results from a “zero-dimensional” (0-D) purely photochemical model and from the SLIMCAT three-dimensional (3-D) chemical transport model over the Plateau de Bure station (45°N, 10°E) from September 1991 to March 1998. A maximum confidence value for the yield in the reaction $\text{ClO} + \text{OH} \rightarrow \text{HCl} + \text{O}_2$ is deduced from the analysis to be in the range $0.05\text{--}0.10 \pm 0.03$, which is consistent with recent laboratory data, suggesting a value of $\sim 0.05\text{--}0.06 \pm 0.02$. Comparisons between the ClO diurnal variations measured by MLS and calculated by the 0-D model agree to within 10% around the maximum of ClO (~40 km) and within 5% elsewhere. The ClO diurnal variation is induced by variations in the partitioning with HOCl and ClONO₂ below 50 km and by variations in the partitioning within the ClO_x (=Cl+ClO) family above. The agreement between measured and modeled seasonal variations of ClO implies an evolution above 30 km essentially dictated by the variation in the partitioning with HCl, together with the partitioning within the ClO_x family above 40 km. The differences between measured and modeled ClO seasonal variations above 50 km are attributed to uncertainties in the relative rates of the sources of HCl (reactions of Cl with CH₄ and HO₂).

1. Introduction

Ozone depletion in the lower stratosphere at high latitudes has been known for more than a decade to be clearly induced by the activation of chlorine compounds (e.g., chlorine monoxide) via heterogeneous reactions in/on polar stratospheric clouds [World Meteorological Organization (WMO), 1995]. In addition, a decrease in

stratospheric column ozone of a few percent per decade is also observed at midlatitudes. Detecting and explaining the temporal evolution of chlorine compounds are prerequisites in helping to interpret the temporal evolution of ozone in the stratosphere.

We decided to use ClO measurements obtained since September 1991 by the Microwave Limb Sounder (MLS) instrument aboard the UARS satellite, to study the diurnal and the seasonal variations of midstratospheric ClO over the northern midlatitudes. To interpret the temporal evolutions, measurements from the Halogen Occultation Experiment (HALOE) and the Cryogenic Limb Array Etalon Spectrometer (CLAES) aboard UARS were also used together with calculations from a purely photochemical zero-dimensional (0-D) model and the SLIMCAT three-dimensional (3-D) chemical transport model.

Measurements from MLS [Barath *et al.*, 1993] are temperature profiles and ClO mixing ratios using level 3AT version 4 files stored on the distributed active archive center (DAAC). Measurements from HALOE [Russell *et al.*, 1993] are O₃, HCl, H₂O, and CH₄ mix-

¹Observatoire de Bordeaux, Centre National de la Recherche Scientifique/Institut National des Sciences de l'Univers, Floirac, France.

²School of the Environment, University of Leeds, Leeds, England, United Kingdom.

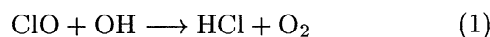
³Jet Propulsion Laboratory, Pasadena, California.

⁴Center for Atmospheric Sciences, Hampton University, Hampton, Virginia.

⁵Lockheed Martin Advanced Technology Center, Palo Alto, California.

ing ratios using level 3AT version 18 files on the DAAC. Measurements from CLAES [Roche *et al.*, 1993] are ClONO₂ and NO₂ mixing ratios using level 3AT version 8 files on the DAAC. Only MLS data flagged with a positive uncertainty that is with an a priori contribution <25% were taken. Satellite data have been averaged within a latitude band from 40° to 50°N irrespective of the sunset or sunrise period of measurement for HALOE, while ClO, ClONO₂, and NO₂ measurements were binned in 24×1 hour wide bins in order to detect diurnal variations. The amount and the quality of UARS data offer a unique opportunity for quantitatively studying the photochemistry of stratospheric compounds. In particular, studies of the diurnal cycle of ClO are appropriate tools for constraining the yield of the ClO + OH reaction, while studies of the ClO seasonal cycles help explore issues related to chlorine partitioning. Trends in ClO over the 1991-1997 time period are studied by Froidevaux *et al.* [this issue].

The 0-D model, described in detail by Ricaud *et al.* [1994, 1996], is initialized with temperature profiles taken from Barnett and Corney [1985] for the month corresponding to the observation period. We verified that the climatological seasonal variation in temperature was consistent with the monthly averaged temperature field as measured by MLS. In order to be as close as possible to the state of the atmosphere as seen by UARS during the 1991-1997 period, (1) we decided to use monthly averaged measurements of O₃, CH₄, H₂O, and HCl from HALOE for the appropriate month; (2) we adjusted the monthly averaged CLAES ClONO₂ values upward by a factor 1.2 as an average compensation for the increasing low bias of these data versus correlative measurements [Mergenthaler *et al.*, 1996] in this high-altitude region of rapidly decreasing ClONO₂ mixing ratio for the appropriate month; and (3) we used a yearly averaged midlatitude climatological atmosphere where chlorine compounds such as ClO, Cl, and HOCl have been rescaled by a factor 1.3 to account for the positive trend of chlorine loading of ~1.1 ppbv decade⁻¹ [WMO, 1995] from the mid-1980s to the mid-1990s, independent of the month. Total inorganic chlorine above 4.6 hPa is ~3.4 ppbv. Climatological NO₂ has been appropriately adjusted in order to overestimate CLAES NO₂ measurements since there is a 20-30% low bias in the NO₂ data for pressures <10 hPa [Reburn *et al.*, 1996; Ricaud *et al.*, 1998]. Outputs are selected for day 15 of each month. Reaction rates are updated from the JPL97 handbook [DeMore *et al.*, 1997]. The yield η of the reaction



is an important issue in the understanding of the temporal evolution of the chlorine budget and related species such as O₃ [see, e.g., Toumi and Bekki, 1993; Lary *et al.*, 1995]. Since recent laboratory measurements by Lipson *et al.* [1997] give $\eta \sim 0.05\text{--}0.06 \pm 0.02$, values of

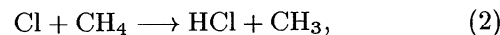
0, 0.05, and 0.1 were given to η in the 0-D model when studying the ClO diurnal variations. When studying the ClO seasonal variations, a value of 0.05 was taken, and two runs were processed. In run A, HCl comes from monthly averaged measurements from HALOE (as described above) adapted to the corresponding month, while in run B, HCl comes from the yearly averaged measurements from HALOE and is thus kept constant throughout the year.

The 3-D model [Chipperfield *et al.*, 1996] uses meteorological analyses to force the circulation and contains a detailed stratospheric chemistry scheme [Chipperfield, 1999]. The model run used here is the same as that described by Ricaud *et al.* [1998] with η set to 0.05, except that model output is sampled at 1200 UT at the Plateau de Bure station (45°N, 10°E). The model run was forced using U.K. Meteorological Office (UKMO) analyses with a horizontal resolution of 3.75°×3.75°. As this 3-D model run was set up to study interannual variability, there are few imposed external variations. For example, the model was run without a trend in total inorganic chlorine and other source gases and with no solar cycle.

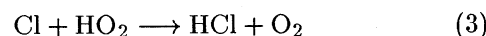
Section 2 presents a general frame relating the ClO temporal evolution to other chlorine compounds. Section 3 deals with the ClO diurnal variations, and section 4 refers to the ClO seasonal variations.

2. Overview of the ClO Temporal Evolution

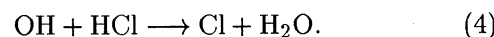
The temporal evolution of ClO is driven by the evolution of other chlorine family constituents (HCl, ClONO₂, HOCl, and Cl) whose importance depends on the time frame and the altitude considered. Early descriptions of the chlorine partitioning were given by Brasseur and Solomon [1984] and Solomon and Garcia [1984], while a more recent study is described by Michelsen *et al.* [1996]. In the middle stratosphere, inorganic chlorine (Cl_y) essentially consists of ~75% of HCl and ~25% of ClO [Zander *et al.*, 1996]. Thus, for time frames greater than a day, ClO evolution is dictated by the slow processes controlling the evolution of HCl, which is produced by



with an important contribution from (1) depending on the yield η , and to a lesser extent in the upper stratosphere, by



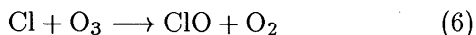
and destroyed through



The Cl/HCl ratio may be written as

$$\frac{[\text{Cl}]}{[\text{HCl}]} \sim \frac{k_4[\text{OH}]}{k_2[\text{CH}_4] + k_3[\text{HO}_2] + k_1[\text{OH}][\text{ClO}]/[\text{Cl}]}, \quad (5)$$

where k_i is the rate constant of reaction (i). Below ~ 40 km, daytime ClO_x ($=\text{Cl}+\text{ClO}$) is mainly ClO with a ratio $\text{Cl}/\text{ClO} \leq 1\%$, while above, the ratio Cl/ClO increases dramatically to $\sim 90\%$ around 55 km. Consequently, above 40 km the evolution of ClO is also governed by the fast processes controlling the partitioning within the ClO_x family, with the main ClO production reaction being



and the main loss reaction being



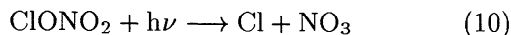
giving a Cl/ClO ratio of

$$\frac{[\text{Cl}]}{[\text{ClO}]} \sim \frac{k_7 [\text{O}]}{k_6 [\text{O}_3]}. \quad (8)$$

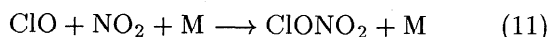
Thus, above 40 km the ratio (ClO/HCl) becomes

$$\frac{[\text{ClO}]}{[\text{HCl}]} \sim \left\{ \frac{k_4 [\text{OH}]}{k_2 [\text{CH}_4] + k_3 [\text{HO}_2] + k_1 [\text{OH}] [\text{ClO}]/[\text{Cl}]} \right\} \times \frac{k_6 [\text{O}_3]}{k_7 [\text{O}]} \quad (9)$$

At altitudes lower than 40 km, ClONO_2 (and, to a lesser extent, HOCl) are not negligible within Cl_y , thus the evolution of ClONO_2 , which is governed by photolysis



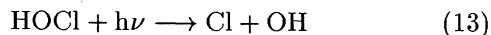
and the production reaction



also plays a role in the ClO evolution when considering a time frame of the order of a day, giving a fast daytime equilibrium

$$\frac{[\text{ClO}]}{[\text{ClONO}_2]} \sim \frac{J_{10}}{k_{11} [\text{NO}_2] [\text{M}]}, \quad (12)$$

where J_i is the photodissociation coefficient of the reaction (i). The evolution of HOCl within a time frame of a day is dictated by the photolysis reaction



and the production reaction



giving a fast daytime equilibrium

$$\frac{[\text{ClO}]}{[\text{HOCl}]} \sim \frac{J_{13}}{k_{14} [\text{HO}_2]}. \quad (15)$$

3. Diurnal Variation

Previous studies [e.g., Solomon *et al.*, 1984; Ricaud *et al.*, 1997] reported diurnal variations of ClO at mid-

latitudes by ground-based millimeter-wave techniques, either as a normalized and integrated amount or within a broad altitude layer of ~ 10 km vertical resolution. These results, although qualitatively important, have a strong quantitative limitation due to the vertical resolution and showed contamination of the retrieval by the a priori information, essentially because the ClO lines at millimeter wavelengths are very weak and very difficult to detect. Indeed, the first diurnal variations in ClO

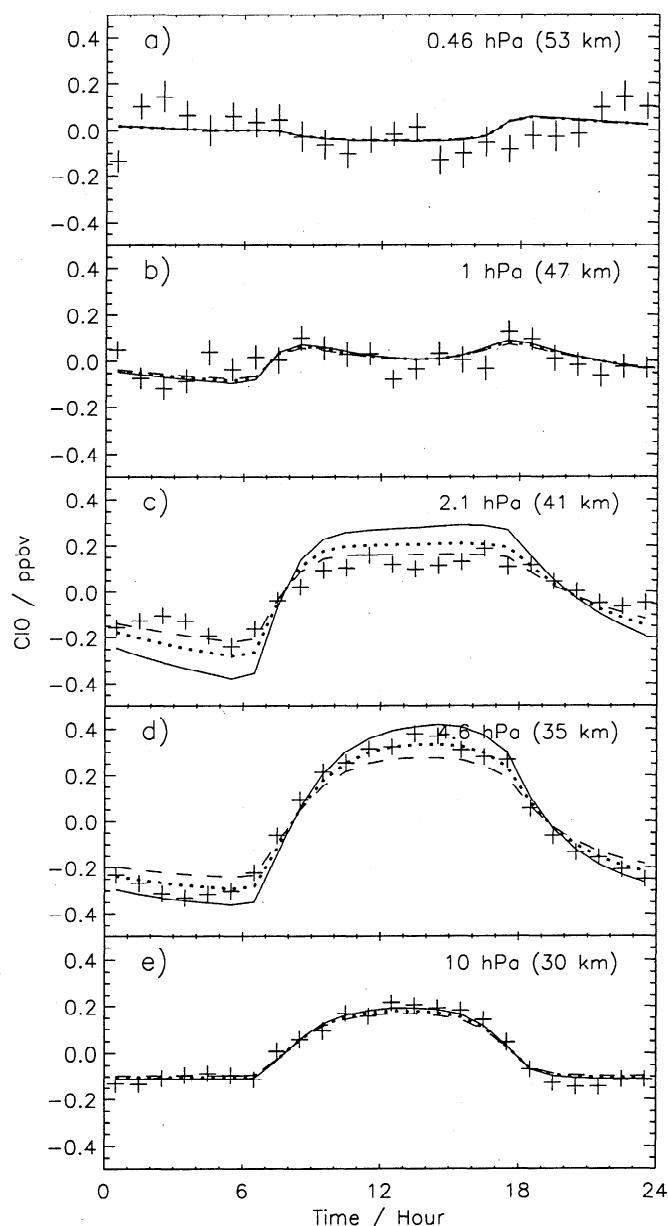


Figure 1. The ClO diurnal variation at (a) 0.46 (~ 53 km), (b) 1 (~ 47 km), (c) 2.1 (~ 41 km), (d) 4.6 (~ 35 km), and (e) 10 hPa (~ 30 km) as measured by UARS/Microwave Limb Sounder (MLS) from 1991 to 1997 within the band 40° - 50°N and averaged irrespective of the year within 24 1 hour wide (crosses) bins and as calculated by a 0-D purely photochemical model with $\eta = 0$ (solid line), 0.05 (dotted line), and 0.1 (dashed line) at 45°N in February. Vertical bars represent a 1σ error.

as measured by UARS/MLS and presented by *Waters et al.* [1996] show very good agreement with variations normalized to unity at noon and about zero at 0400 local solar time (LST) as calculated by the model of *Ko and Sze* [1984] and as published by *Solomon et al.* [1984].

Midstratospheric ClO diurnal variations are shown in Figure 1 at 10 (~31 km), 4.6 (~36 km), 2.1 (~42 km), 1 (~47 km), and 0.46 hPa (~53 km). Because of the low bias of nighttime ClO values in MLS reported by *Waters et al.* [1996], diurnal amplitudes are evaluated as the diurnal variation minus the 24 hour average value. Using a method described by *Ricaud et al.* [1996], MLS data (crosses) have been monthly averaged within the latitude band 40°-50°N irrespective of the year from

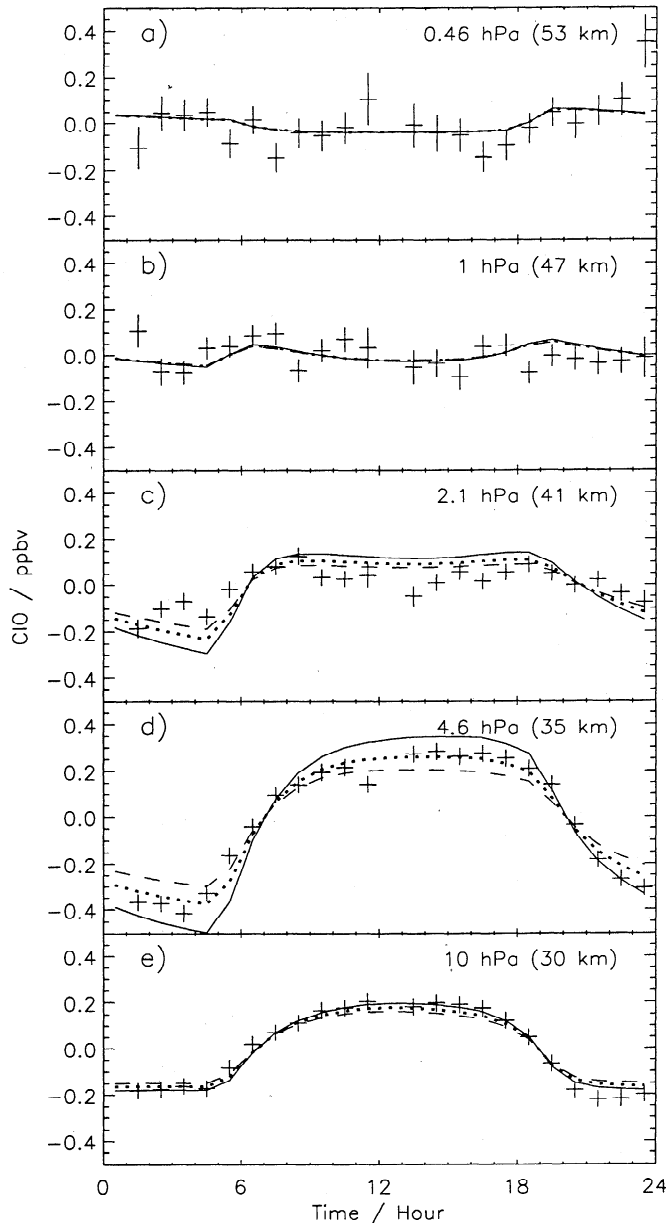


Figure 2. Same as Figure 1 but in May.

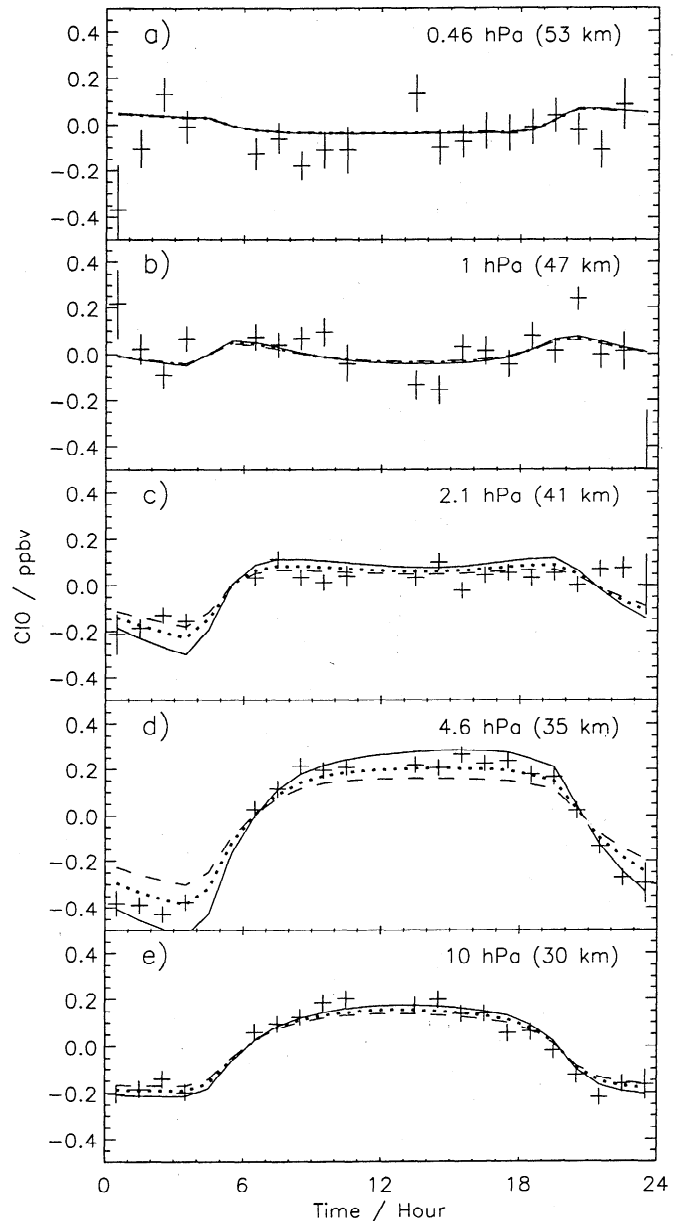


Figure 3. Same as Figure 1 but in July.

1991 to 1997 during the month of February in 24×1 hour wide bins. Error bars are representative of the 1 σ error. The 0-D model outputs are evaluated for February 15 with η equal to 0 (solid line), 0.05 (dotted line), and 0.1 (dashed line). The original model temporal resolution of 10 min has been degraded to 1 hour. The change of ClO diurnal cycle with season can be seen as measured and calculated in May, July, and October in Figures 2, 3 and 4, respectively, with a decrease in amplitude from winter to summer as day length increases.

Within all layers from 10 to 2.1 hPa where there is a significant amount of ClO, the modeled amplitude decreases with η since reaction (1) is a sink for ClO_x. The difference in amplitudes calculated with $\eta=0-0.1$ may be as large as ± 0.12 ppbv at 4.6 hPa (Figures 1d, 2d, 3d, and 4d). If we consider quantitatively the amplitudes

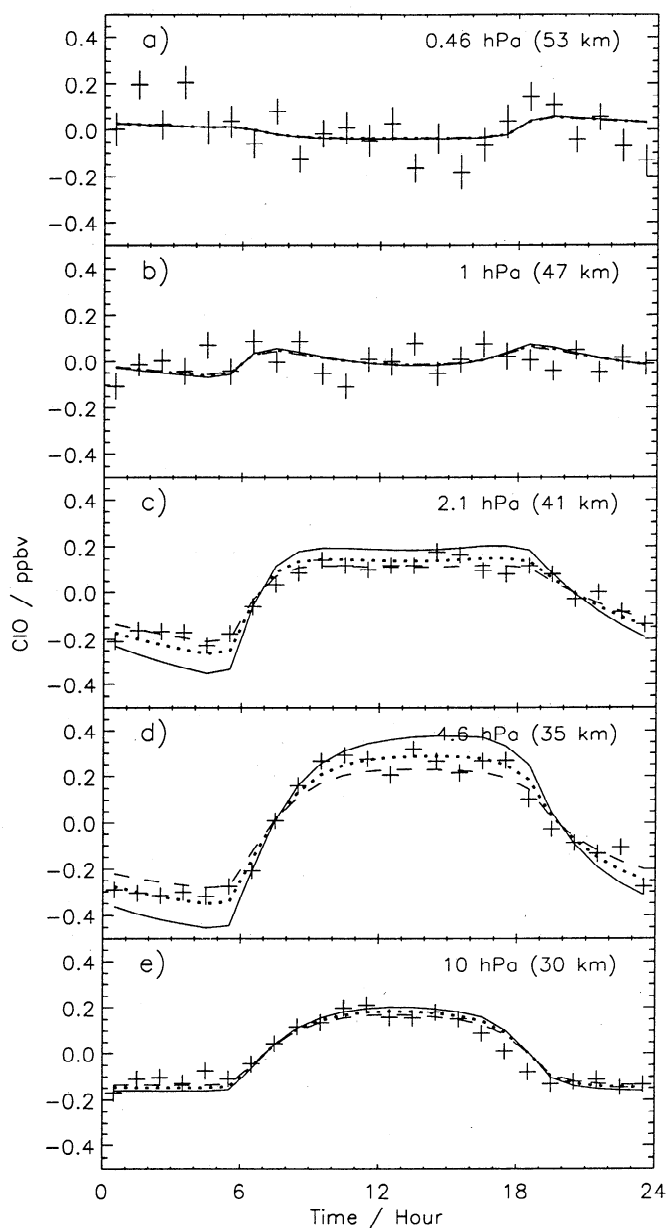


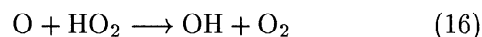
Figure 4. Same as Figure 1 but in October.

of the diurnal variations, we find very good agreement between measurements and models at 10 hPa (Figures 1e, 2e, 3e, and 4e) to within 0.02 ppbv ($\sim 5\%$). The difference between the three modeled amplitudes is <0.01 ppbv. At 4.6 hPa (Figures 1d, 2d, 3d, and 4d), the measured amplitude lies around those calculated for $\eta=0.05$. At 2.1 hPa (Figures 1c, 2c, 3c, and 4c) the measured amplitudes tend to be of the order of, or even smaller than, the amplitude calculated even with $\eta=0.1$. At 1 hPa (Figures 1b, 2b, 3b, and 4b), 1σ error bars reach ~ 0.05 ppbv ($\sim 10\%$), but the agreement between model and measurement is reasonable. The slight ClO minimum at noon is clearly seen in February (Figure 1b) and in October (Figure 4b). At 0.46 hPa (Figures 1a, 2a, 3a, and 4a), although measurement errors are ~ 0.07 ppbv, the night-to-day decrease in ClO is observed in the four

periods with a measured amplitude that appears to be slightly greater than those modeled in February (Figure 1a) and October (Figure 4a). Our analysis of the amplitude of the ClO diurnal variations tends to show that the maximum confidence value for η is within the range 0.05–0.1, which is consistent with recent laboratory data suggesting a value of $\sim 0.05\text{--}0.06 \pm 0.02$.

The diurnal variation of ClO depends upon the absolute amounts of ClO_x , NO_2 , and HO_2 (see below). We estimate that the amount of ClO_x in the 0-D model is known with an uncertainty of $\sim 10\%$ and that it is related to (1) the adjustment of the modeled Cl, ClO, and HOCl amounts from the mid-1980s to the mid-1990s and (2) the uncertainty in the HCl and ClONO_2 measurements from UARS. We checked that the amplitude of the ClO diurnal variation linearly responded to a change in ClO_x . Since the maximum of the amplitude is in the vertical range 2.1–4.6 hPa, a 10% error in the amplitude gives an error of $\sim 0.03\text{--}0.04$ ppbv in ClO. Consequently, the associated error upon η does not exceed 0.02. Errors upon NO_2 essentially affect ClO below 2.1 hPa. Assuming a 20% error on NO_2 produces a change in the ClO diurnal variation of $<2\%$ and, consequently, gives a negligible effect upon the estimation of η . The amplitude of the diurnal variation of ClO is found to be insensitive to HO_2 since a 50% change in HO_2 produces a change in the amplitude of ClO of $<1\%$.

We also performed sensitivity studies of the ClO diurnal amplitude with respect to two reactions. First, as discussed by Siskind *et al.* [1998] and Khosravi *et al.* [1998], we decreased the reaction rate of



by 40% in order to reconcile the well known middle to upper stratosphere “ozone deficit problem” [see, e.g., Eluszkiewicz and Allen, 1993] for which the abundance of the modeled ozone is underestimated compared to observations. The net effect upon the ClO diurnal amplitude is at most 0.02 ppbv at 4.6 and 2.1 hPa and almost negligible elsewhere (not shown). Consequently, the associated error upon η might be estimated to be ~ 0.01 . Second, the 0-D model assumes that 2% of the reaction $\text{ClO} + \text{HO}_2$ forms $\text{HCl} + \text{O}_3$ [Finkbeiner *et al.*, 1995], but this nonzero yield has no effect upon the ClO diurnal amplitude whichever layer is considered (not shown). Finally, the error budget associated with the ClO diurnal variations shows that the overall uncertainty upon the value of η does not exceed 0.03.

Over a time frame of 24 hours the ClO temporal variation is no longer dictated by an evolution in the ClO/HCl ratio since the HCl chemical lifetime is ~ 1 day [Brasseur and Solomon, 1984] but rather is dictated by an evolution in the ClO/ ClONO_2 and ClO/HOCl ratios in the middle stratosphere and by partitioning within the ClO_x family in the upper stratosphere. Indeed, Figure 5 shows the diurnal variations of ClO (solid

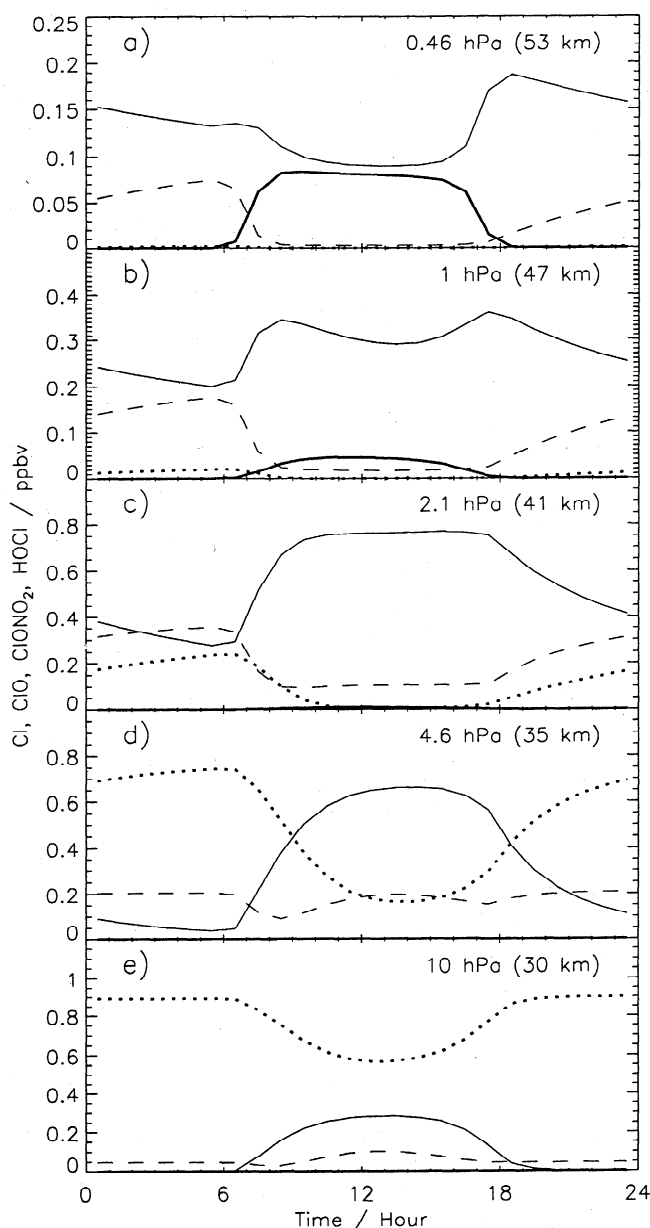


Figure 5. Diurnal variations of ClO (solid line), ClONO₂ (dotted line), HOCl (dashed line), and Cl (thick line) as calculated by the 0-D photochemical model at 45°N in February at (a) 0.46 (~53 km), (b) 1 (~47 km), (c) 2.1 (~41 km), (d) 4.6 (~35 km), and (e) 10 hPa (~30 km).

line), ClONO₂ (dotted line), HOCl (dashed line), and Cl (thick line) calculated by the 0-D model at 10 (~31 km), 4.6 (~36 km), 2.1 (~42 km), 1 (~47 km), and 0.46 hPa (~53 km). The night-to-day increase in ClO is attributed below 40 km to the diurnal variation in ClONO₂ and between 40 and 50 km to variations in HOCl. At 40 km the diurnal variations of both ClONO₂ and HOCl influence the ClO evolution. Above 50 km the ClO variation is no longer anticorrelated with HOCl since it shows a night-to-day decrease that is mainly due to a repartitioning within the ClO_x family proportional to the O/O₃ ratio as mentioned in section 2.

During the night, sink reactions largely dominate source reactions, causing ClO to decrease from sunset to sunrise. For nighttime conditions below 40 km the dominant sink reaction is (11) with a turnover above 40 km where reaction (14) dominates. For daytime conditions at 30 km (see, e.g., Figures 1e and 5e) from sunrise to noon the ClONO₂ photodissociation (10) enables ClO to increase before reaction (14) dominates, explaining the symmetrical variation in ClO with respect to noon. At 35 km (see, e.g., Figures 1d and 5d), from sunrise to ~1000 LST, source reaction (10) dominates, thus ClO increases before the equilibrium between the sink reaction (14) and the source reaction (13) is reached. After ~1600 LST, sink reaction (11) dominates, and ClO decreases. At ~40 km (see, e.g., Figures 1c and 5c), ClO rapidly increases at sunrise from 0600 to 0800 LST because of the rapid photodissociation of HOCl and ClONO₂. Then equilibrium is reached between sink reaction (14) and source reactions (13) and (4). At ~47 km (see, e.g., Figures 1b and 5b) the ClO diurnal variation is no longer completely governed by the source and sink reactions of ClO_x. The Cl/ClO ratio is not negligible and is proportional to O/O₃. Since the ClO diurnal variation also depends on the diurnal variation of O_x (=O+O₃), whose amplitude of night-to-day decrease increases with height [Ricaud *et al.*, 1994], the ClO night-to-day increase amplitude tends to be reduced. Although daytime source reactions (13) and (4) dominate sink reaction (2), a slight decrease in ClO is detected around noon. At 53 km (see, e.g., Figures 1a and 5a), source and sink daytime reactions are similar to the ones listed for 47 km with source reactions much greater than sink reactions. However, the O/O₃ ratio increase produces a net night-to-day decrease in ClO that is mainly due to a repartitioning within the ClO_x family.

4. Seasonal Variation

Data sets $x(t)$, where x represents the constituent mixing ratio or temperature and t is time, available since 1991 from the UARS/MLS, the UARS/HALOE, and the UARS/CLAES instruments and from the 0-D and 3-D models have been decomposed as

$$x(t) = a_0 + a_1 \sin\left(\frac{2\pi}{12}t + a_2\right) + a_3 \sin\left(\frac{2\pi}{6}t + a_4\right) + a_5 t \quad (17)$$

to evaluate the 6 year average value a_0 , the amplitude a_1 and phase a_2 of the annual oscillation, the amplitude a_3 and phase a_4 of the semiannual oscillation, and the long-term trend a_5 , which is naturally not available for the 0-D data set. The long-term trend figures will not be discussed in the present manuscript. Note, for CLAES, only 2 years of data are available. Figure 6 shows the seasonal variations (i.e., the a_1 , a_2 , a_3 , and a_4 terms) of daytime ClO at 10, 4.6, 2.1, 1, and 0.46 hPa

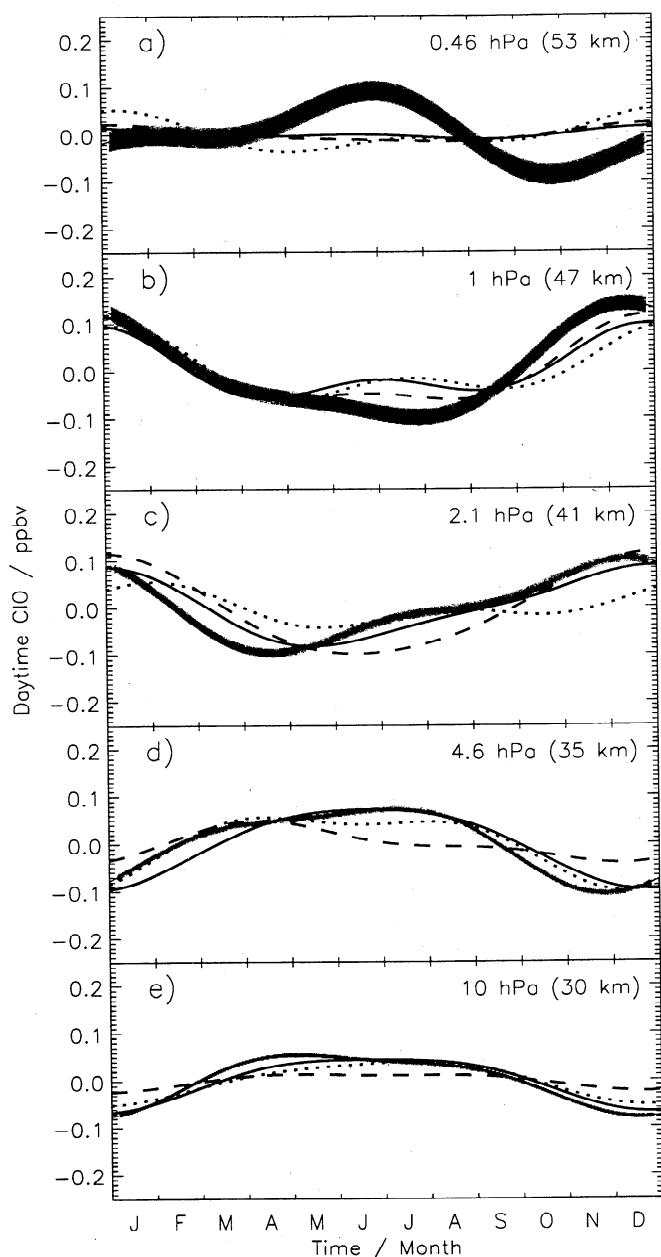


Figure 6. Seasonal variations of daytime ClO as measured by UARS/MLS (thin line) from 1991 to 1997 within the band 40° - 50° N, and as calculated by the run A (thick solid line) and the run B (thick dashed line) 0-D model at 45° N for the 15th day of each month and as calculated by the 3-D SLIMCAT chemical transport model (dotted line) above the station of Plateau de Bure (45° N, 10° E) at 1200 UT at the pressure levels (a) 0.46, (b) 1, (c) 2.1, (d) 4.6, and (e) 10 hPa. Daytime MLS ClO is an average of data measured from 1100 to 1600 local solar time (LST). The shaded area represents the 1σ error domain of the measured ClO seasonal variations.

as measured by MLS and as calculated by the 0-D and 3-D models. Daytime ClO measured by MLS and calculated by the 0-D model are an average of data from 1100 to 1600 LST, while daytime ClO from the 3-D model is valid for 1200 UT. The shaded area represents the 1σ error domain around the measured variation. For

the 0-D model, two runs were performed: run A, using monthly averaged HALOE HCl for the corresponding month; and run B, using yearly averaged HALOE HCl.

At 10 hPa (Figure 6e) the ClO seasonal variations (annual and semiannual oscillations) measured by MLS and calculated by the run A 0-D model and the 3-D model tend to agree both in amplitude (~ 0.075 ppbv) and in phase with a minimum in winter and a broad maximum in spring-summer, although the run B 0-D model seasonal amplitude is almost negligible (≤ 0.01 ppbv). At 4.6 hPa (Figure 6d), there is an overall agreement between MLS, the 3-D model, and the run A 0-D model data with a seasonal amplitude of ~ 0.1

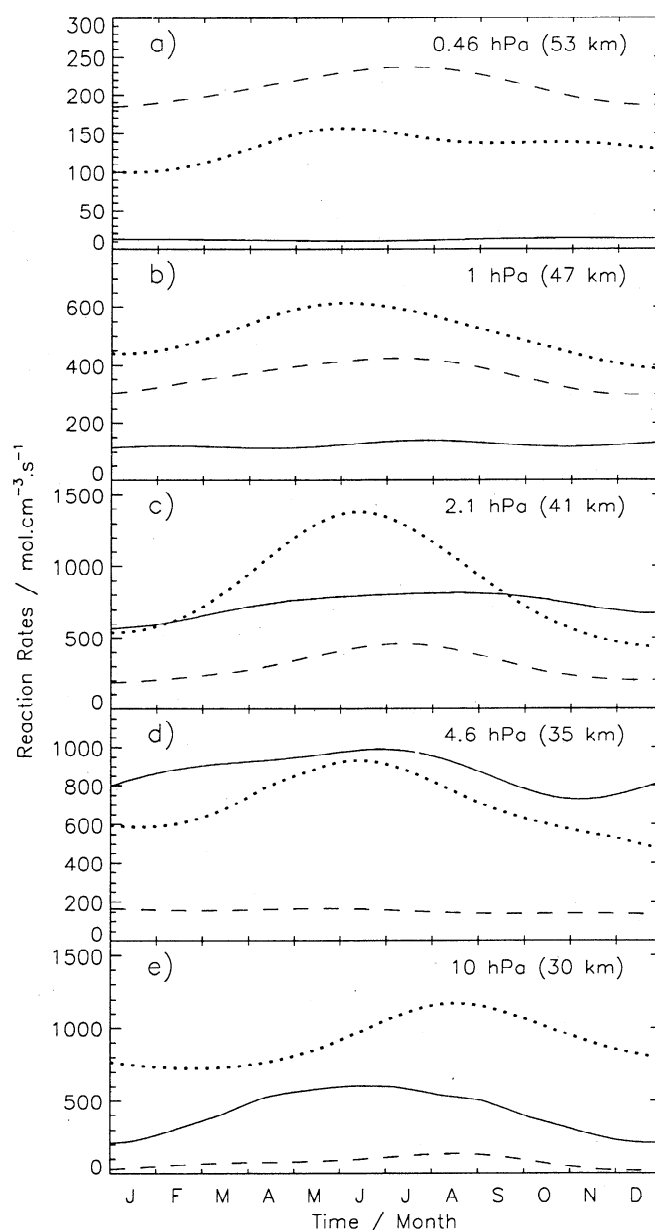


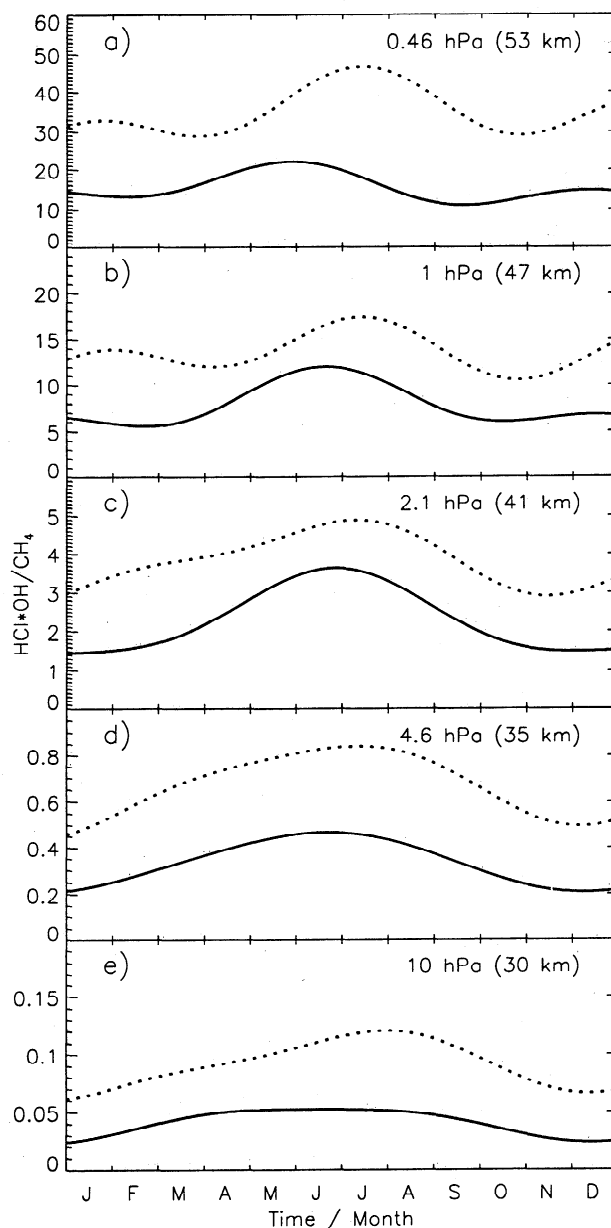
Figure 7. Seasonal variations of the rate (molecules $\text{cm}^{-3}\cdot\text{s}^{-1}$) of the reactions $\text{ClO} + \text{OH} \rightarrow \text{HCl} + \text{O}_2$ (solid line), $\text{Cl} + \text{CH}_4 \rightarrow \text{HCl} + \text{CH}_3$ (dotted line), and $\text{Cl} + \text{HO}_2 \rightarrow \text{HCl} + \text{O}_2$ (dashed line) as calculated by the 0-D model at the pressure levels (a) 0.46, (b) 1, (c) 2.1, (d) 4.6, and (e) 10 hPa.

Table 1. Parameters and Associated Definitions Used in the Text for Interpreting the ClO Seasonal Variations

Parameter	Definition
r_1	$[\text{HCl}] k_4/k_1$
r_1^0	$r_1[\text{O}_3]/[\text{O}]$
r_2	$[\text{HCl}][\text{OH}]/[\text{CH}_4]$
r_2^0	$r_2[\text{O}_3]/[\text{O}]$
r_3	$[\text{HCl}][\text{OH}]/[\text{HO}_2]$
r_3^0	$r_3[\text{O}_3]/[\text{O}]$

ppbv and with minima in winter and maxima in spring-summer, while the run B ClO seasonal variation has a much stronger semiannual oscillation. At 2.1 hPa (Figure 6c) the amplitude of the 3-D seasonal variation is weaker by ~ 0.05 ppbv than that measured and that calculated by the run A 0-D model. The measured ClO evolution compares well with the run A 0-D model, with an amplitude of ~ 0.1 ppbv, a minimum in spring, and a maximum in winter, although the run B 0-D model variation has a strong annual component, with a maximum in winter and a minimum in summer. At 1 hPa (Figure 6b) all data sets show a winter to summer decrease of ~ 0.1 ppbv; however, the deep minimum in summer as deduced from measurements is not captured by any model. Interestingly, all modeled variations have similar patterns with a marked semiannual oscillation. Finally, at 0.46 hPa (Figure 6a), there is a strong disagreement between models and observations both in amplitude and phase. The modeled amplitude is very weak (~ 0.02 ppbv), although it reaches ~ 0.1 ppbv in MLS data. Also, models tend to show a winter-to-summer decrease, although MLS data exhibit a marked semiannual oscillation with a strong maximum in summer and a deep minimum in fall. Even if, at this pressure layer, errors associated with MLS measurements are ~ 0.03 ppbv, i.e., bigger than the ones at higher pressures (~ 0.01 ppbv), the measurement-model difference appears to be significant.

If we exclude the 0.46 hPa layer, measured ClO seasonal variations agree systematically much better with variations calculated with the run A 0-D model than with the run B 0-D model. Indeed, as mentioned in section 2, the ClO evolution over a time frame much greater than a day is dictated in the middle and upper stratosphere by the evolution of HCl [Solomon and Garcia, 1984]. The three main reactions producing HCl above 30 km are (1), (2), and (3). By setting $\eta=0.05$ for (1), Figure 7 shows the seasonal evolution in reaction rates of (1) (solid line), (2) (dotted line), and (3) (dashed line) as calculated by the 0-D model at 10, 4.6, 2.1, 1, and 0.46 hPa. At 10 hPa, (2) is the main production reaction of HCl, even assuming that 2% of the reaction $\text{ClO} + \text{HO}_2$ forms $\text{HCl} + \text{O}_3$. Between 4.6 and 2.1 hPa both (1) and (2) play a key role

**Figure 8.** Seasonal variations of the ratio $r_2 = [\text{HCl}][\text{OH}]/[\text{CH}_4]$ as calculated by the 0-D model (thick line) and by the 3-D SLIMCAT chemical transport model (dotted line) at the pressure levels (a) 0.46, (b) 1, (c) 2.1, (d) 4.6, and (e) 10 hPa.

in producing HCl, while (3) starts being nonnegligible. At 1 and 0.46 hPa, (2) and (3) are the dominant reactions, while (1) is becoming negligible with increasing height. Using (5) and (9), ClO evolution depends on the evolution of the ratios $r_1 = [\text{HCl}]k_4/k_1$, $r_2 = [\text{HCl}][\text{OH}]/[\text{CH}_4]$, and $r_3 = [\text{HCl}][\text{OH}]/[\text{HO}_2]$, which need to be scaled by $[\text{O}_3]/[\text{O}]$ in the upper stratosphere, giving $r_1^0 = r_1[\text{O}_3]/[\text{O}]$, $r_2^0 = r_2[\text{O}_3]/[\text{O}]$, and $r_3^0 = r_3[\text{O}_3]/[\text{O}]$ (Table 1). More precisely, ClO evolution in the middle stratosphere must then follow the evolution of r_1 and r_2 , and in the upper stratosphere, ClO depends on both r_2^0 and r_3^0 . Interestingly, the r_1 seasonal variation

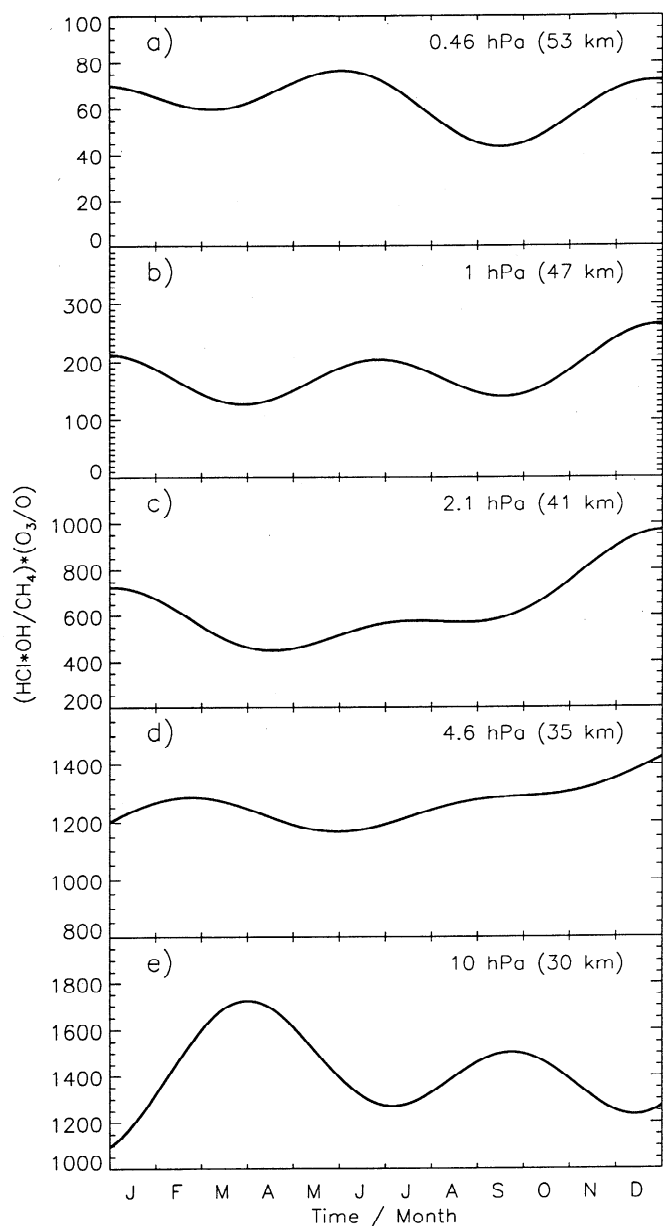


Figure 9. Seasonal variations of the ratio $r_2^0 = [\text{HCl}][\text{OH}]/[\text{CH}_4] \times [\text{O}_3]/[\text{O}]$ as calculated by the 0-D model (thick line) at the pressure levels (a) 0.46, (b) 1, (c) 2.1, (d) 4.6, and (e) 10 hPa.

(not shown) plays a negligible role in the ClO seasonal variation (even taking into account the temperature dependence in k_4/k_1) since the reactions (1) and (4) essentially produce an equilibrium process between ClO and HCl via OH as both source and sink.

Figures 8, 9, and 10 show the seasonal variations of the quantities r_2 , r_2^0 , and r_3^0 as calculated by the run A 0-D model at 10, 4.6, 2.1, 1, and 0.46 hPa, respectively. Note that r_2 as calculated by the 3-D model is also shown in Figure 8 and behaves similarly, although greater, than the one calculated by the 0-D model. This is due to the fact that CH_4 calculated by SLIMCAT is less than the HALOE measurements used to constrain

the 0-D model. Below 40 km the modeled quantities have a strong annual oscillation with maxima in summer and minima in winter and a more pronounced semi-annual oscillation above. The shape of the variations of r_2 at 10 (Figure 8e) and 4.6 hPa (Figure 8d) agree with the ClO variations. At 2.1 hPa (Figure 8c) the variations of r_2 is out of phase compared to those for ClO. Indeed, at and above this pressure layer, partitioning within the ClO_x is no longer negligible, thus the seasonal evolution of r_2^0 (Figure 9c) compares very well with the evolution of ClO measured by MLS and calculated by the 3-D and the run A 0-D models. At 1 hPa, ClO evolution depends on CH_4 , HO_2 , and ClO_x . The

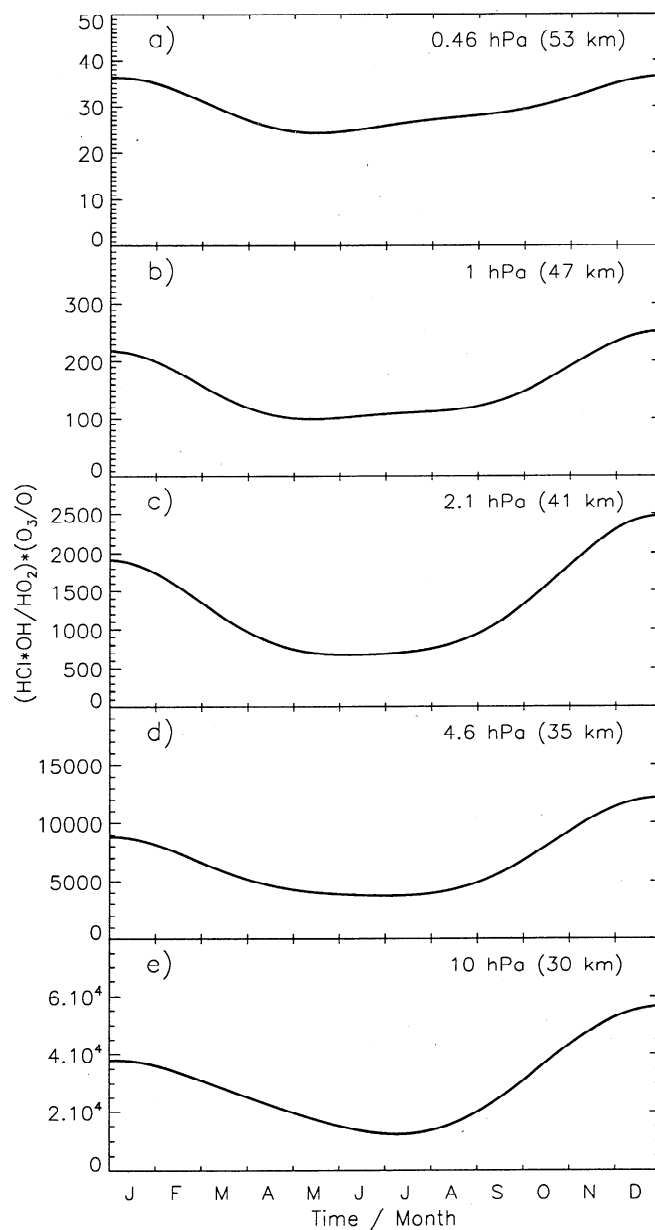


Figure 10. Seasonal variations of the ratio $r_3^0 = [\text{HCl}][\text{OH}]/[\text{HO}_2] \times [\text{O}_3]/[\text{O}]$ as calculated by the 0-D model (thick line) at the pressure levels (a) 0.46, (b) 1, (c) 2.1, (d) 4.6, and (e) 10 hPa.

r_2^0 evolution (Figure 9b) shows the typical semiannual oscillation seen on the modeled ClO variations, while the measured ClO variation has a more pronounced annual oscillation that is the signature of the r_3^0 evolution (Figure 10b). At 0.46 hPa, where the discrepancy between measured and modeled ClO is the largest, the measured ClO evolution compares well with the evolution of r_2^0 (Figure 9a), while the modeled ClO variation tends to follow the r_3^0 evolution (Figure 10a). Consequently, the differences between modeled and measured ClO seasonal variations in the upper stratosphere can be attributed to model errors in the relative strength between the HCl source reactions ($\text{Cl} + \text{CH}_4$ and $\text{Cl} + \text{HO}_2$).

Finally, we can note from (12) that although ClONO_2 is in equilibrium with ClO during the daytime, the ClO/ ClONO_2 partitioning dependence on NO_2 can also govern the ClO seasonal cycle. Since we used ClONO_2 and NO_2 measurements from UARS, we verified that the ClONO_2 partitioning is a second-order effect compared to the HCl partitioning upon the ClO seasonal evolution.

5. Conclusions

This analysis has presented the temporal evolution of middle to upper stratospheric ClO from 10 to 0.46 hPa ($\sim 30\text{--}55$ km) over 24 hours (diurnal variations) and over 1 year (seasonal variations) at northern midlatitudes as measured by the UARS/MLS instrument and as calculated by 0-D and 3-D models. We have used the unique opportunity of UARS measurements to study the diurnal cycle of ClO and to deduce that the yield in the reaction $\text{ClO} + \text{OH} \rightarrow \text{HCl} + \text{O}_2$ ranges from $0.05\text{--}0.10 \pm 0.03$, which is consistent with recent laboratory data suggesting a value of $0.05\text{--}0.06 \pm 0.02$. The diurnal variation of ClO is attributed below 50 km to an evolution in the partitioning with HOCl and ClONO_2 , producing a night-to-day increase in ClO, while above 50 km, it is determined by a change in the partitioning within the ClO_x family: a night-to-day decrease in ClO is observed and calculated in the upper stratosphere at 0.46 hPa (~ 53 km). The UARS measurements have also helped to characterize partitioning issues on a time frame >1 month. The seasonal evolution of ClO is essentially driven by the evolution of HCl below 40 km, while above, the evolution of the partitioning within the ClO_x family becomes more and more important with height. Model errors in the relative strength between sources of HCl in the upper stratosphere ($\text{Cl} + \text{CH}_4$ and $\text{Cl} + \text{HO}_2$) may explain some differences between measured and modeled ClO seasonal variations above 50 km.

Acknowledgments. The authors would like to thank the referees for their very helpful comments. The authors acknowledge many colleagues who have contributed to the MLS, HALOE, and CLAES experiments (in particular, NA-

SA and the UARS project office) and the U.K. Meteorological Office for the meteorological data. One author (PR) would like to thank C. Boone at IPSL, Paris, France, for getting UARS data from the DAAC to ETHER, the French atmospheric database (<http://ether.ipsl.jussieu.fr>). This project has been funded in France by the CNRS/INSU, the CNES, and the MENRT. The modeling work at Leeds was supported by the U.K. Natural Environment Research Council.

References

- Barath, F., et al., The Upper Atmosphere Research Satellite Microwave Limb Sounder instrument, *J. Geophys. Res.*, **98**, 10,751-10,762, 1993.
- Barnett, J. J., and M. Corney, Middle atmosphere reference model derived from satellite data, in *Middle Atmosphere Program*, vol. 16, pp. 47-85, SCOSTEP Sec., Univ. of Ill., Urbana, 1985.
- Brasseur, G., and S. Solomon, *Aeronomy of the Middle Atmosphere: Chemistry and Physics in the Stratosphere and Mesosphere*, D. Reidel, Norwell, Mass., 1984.
- Chipperfield, M. P., Multiannual simulations with a three-dimensional chemical transport model, *J. Geophys. Res.*, **104**, 1781-1805, 1999.
- Chipperfield, M. P., et al., Analysis of UARS data in the southern polar vortex in September 1992 using chemical transport model, *J. Geophys. Res.*, **101**, 18,861-18,881, 1996.
- DeMore, W. B., et al., Chemical kinetics and photochemical data for use in stratospheric modeling, *Publ. 97-4*, Jet Propul. Lab., Pasadena, Calif., 1997.
- Eluszkiewicz, J., and M. Allen, A global analysis of the ozone deficit in the upper stratosphere and lower mesosphere, *J. Geophys. Res.*, **98**, 1069-1082, 1993.
- Finkbeiner, M., et al., Reaction between HO_2 and ClO: Product formation between 210 and 300 K, *J. Phys. Chem.*, **99**, 16,264-16,275, 1995.
- Froidevaux, L., J. W. Waters, W. G. Read, P. S. Connell, D. E. Kinnison, and J. M. Russell III, Variations in the free chlorine content of the stratosphere (1991-1997): Anthropogenic, volcanic, and methane influences, *J. Geophys. Res.*, this issue.
- Khosravi, R., et al., Significant reduction in the stratospheric ozone deficit using a three-dimensional model constrained with UARS data, *J. Geophys. Res.*, **103**, 16,203-16,219, 1998.
- Ko, M. K. W., and N. D. Sze, Diurnal variation of ClO: Implications for the stratospheric chemistries of ClONO_2 , HOCl, and HCl, *J. Geophys. Res.*, **89**, 11,619-11,632, 1984.
- Lary, D. J., M. P. Chipperfield, and R. Toumi, The potential impact of the reaction $\text{OH} + \text{ClO} \rightarrow \text{HCl} + \text{O}_2$ on polar ozone photochemistry, *J. Atmos. Chem.*, **21**, 61-79, 1995.
- Lipson, J. B., et al., Temperature dependence of the rate constant and branching ratio for the $\text{OH} + \text{ClO}$ reaction, *J. Chem. Soc. Faraday Trans.*, **93**, 2665-2673, 1997.
- Mergenthaler, J. L., et al., Validation of CLAES ClONO_2 , *J. Geophys. Res.*, **101**, 9603-9620, 1996.
- Michelsen, H. A., et al., Stratospheric chlorine partitioning: Constraints from shuttle-borne measurements of [HCl], [ClONO_2], and [ClO], *Geophys. Res. Lett.*, **23**, 2361-2364, 1996.
- Reburn, W. J., et al., Validation of nitrogen dioxide measurements from the Improved Stratospheric and Mesospheric Sounder, *J. Geophys. Res.*, **101**, 9873-9895, 1996.
- Ricaud, P., et al., Theoretical validation of ground-based microwave ozone observations, *Ann. Geophys.*, **12**, 664-673, 1994.

- Ricaud, P., et al., Diurnal variability of mesospheric ozone as measured by the UARS Microwave Limb Sounder instrument: Theoretical and ground-based validations, *J. Geophys. Res.*, *101*, 10,077-10,089, 1996.
- Ricaud, P., J. de La Noë, R. Lauqué, and A. Parrish, Analysis of stratospheric chlorine monoxide measurements recorded by a ground-based radiometer located at the Plateau de Bure, France, *J. Geophys. Res.*, *102*, 1423-1439, 1997.
- Ricaud, P., et al., Stratosphere over Dumont d'Urville, Antarctica, in winter 1992, *J. Geophys. Res.*, *103*, 13,267-13,284, 1998.
- Roche, A. E., et al., The Cryogenic Limb Array Etalon Spectrometer (CLAES) on UARS: Experiment description and performance, *J. Geophys. Res.*, *98*, 10,763-10,775, 1993.
- Russell, J. M., et al., The Halogen Occultation Experiment, *J. Geophys. Res.*, *98*, 10,777-10,797, 1993.
- Siskind, D. E., L. Froidevaux, J. M. Russell, and J. Lean, Implications of upper stratospheric trace constituent changes observed by HALOE for O₃ and ClO from 1992 to 1995, *Geophys. Res. Lett.*, *25*, 3513-3516, 1998.
- Solomon, P. M., R. de Zafra, A. Parrish, and J. W. Barrett, Diurnal variation of chlorine monoxide: A critical test of chlorine chemistry in the ozone layer, *Science*, *224*, 1210-1214, 1984.
- Solomon, S., and R. R. Garcia, On the distributions of long-lived tracers and chlorine species in the middle atmosphere, *J. Geophys. Res.*, *89*, 11,633-11,644, 1984.
- Toumi, R., and S. Bekki, The importance of the reactions between OH and ClO for stratospheric ozone, *Geophys. Res. Lett.*, *20*, 2447-2450, 1993.
- Waters, J. W., et al., Validation of UARS Microwave Limb Sounder ClO measurements, *J. Geophys. Res.*, *101*, 10,091-10,127, 1996.
- World Meteorological Organization (WMO), Scientific assessment of ozone depletion: 1994, *Rep. 37*, Geneva, Switzerland, 1995.
- Zander, R., et al., The 1994 northern midlatitude budget of stratospheric chlorine derived from ATMOS/ATLAS-3 observations, *Geophys. Res. Lett.*, *23*, 2357-2360, 1996.
-
- M. P. Chipperfield, School of the Environment, University of Leeds, Leeds LS2 9JT, England, U.K.
- P. Ricaud, Observatoire de Bordeaux, CNRS/INSU, BP 89, 33270, Floirac, France. (ricaud@observ.u-bordeaux.fr)
- A. E. Roche, Lockheed Martin Advanced Technology Center, Palo Alto, CA 94303.
- J. M. Russell III, Center for Atmospheric Sciences, Hampton University, P.O. Box 6075, 23 Tyler Street, Hampton, VA 23668.
- J. W. Waters, Jet Propulsion Laboratory, Mail Stop 103-701, 4800 Oak Grove Drive, Pasadena, CA 91109.

(Received February 9, 1999; revised September 20, 1999; accepted September 23, 1999.)